

Effects of internal heat generation/absorption on heat transfer in a porous enclosure

Najib Hdhiri *, Brahim Ben-Beya, Taieb Lili

Laboratory of Fluid Dynamics, Physics Department, Faculty of Sciences of Tunis, Campus Universitaire, 2092 El-Manar II, Tunisia

Abstract: The present investigation deals with study of laminar natural convection flow with internal heat generation or absorption in porous enclosure. The numerical simulations were conducted using a numerical approach based on the finite volume method implemented in the code "Nasim". It is interesting to see that the internal heat generation numbers (Ra_f), Darcy number (Da) and porosity number (ϵ), have a significant role in the heat transfer rate. For all values of the considered Da , the stream function maximum (ψ_{max}) is found to increase as Da increases. On other hand, at higher value of ($\epsilon=1$), the transfer rate of the heat is so strong which causes a deviation of the heat source maximum temperature corresponding to the absorption case.

Key words: Porous medium, heat generation/absorption.

1. Introduction

Phenomena of convective flows through porous media received a great deal of attention during the last four decades, mainly due to a broad range of applications in science and technology such as fluid flow in geothermal reservoirs, thermal insulation engineering, separation process, petroleum reservoirs, nuclear reactors etc. The literature concerning convective flows in porous media is given elsewhere such the books of Ingham and Pop [1], Vafai [2], Nield and Bejan [3], and others. Many studies involve the extended Darcy model, for instance, Forchheimer and Brinkman extensions [4] are widely used to take into account porous media effects especially for high velocity values and high porosity. Natural convection in a square enclosure filled with a fluid saturated porous medium has been investigated for Brinkman-extended Darcy flow [5], and for Darcy flow [6]. Several situations where non-Darcian effects and viscous effect are dominant, further

extensions are required to Darcy law. In fact, two distinguished modifications to Darcy law are considered namely Brinkmans and Forchheimers models [7]. Many investigations were undertaken on natural convection within porous square enclosures. Sankar et al. provided an analysis of the convective flow and heat transfer in a square porous cavity with partially active thermal walls. Alloui et al. [8] carried out an investigation to study the natural convection flows within a square cavity filled with binary fluid saturated porous media where some portion of the bottom surface is isothermally heated while the upper surface is maintained at constant cold temperature and all other surfaces are adiabatic. Mearly and Merkin [9] investigated the internal heat generation effects on convective flow within a square region filled with a fluid-saturated porous medium. Their results show that the internal heating, particularly for the larger values of the heating parameter, can significantly generate higher temperatures. Furthermore, for larger values of Ra , the internal heating becomes confined mainly to the upward flowing boundary layer on the heated wall and

* **Corresponding author:** Najib Hdhiri
E-mail: hdhiri_najib@yahoo.fr.

its overall effect is reduced. Reddy and Narasimhan [10] analysed numerically the interplay between internal heat generation and externally driven natural convection inside a porous medium annulus. They argued that beyond a critical heat generation value, the unicellular convection pattern present due to the external temperature difference evolves into a bicellular convection. They also proposed a correlation between RaI and RaE and Da to predict the cold end, fluid based and Nusselt number.

To the best of our knowledge, natural convection in porous medium with internal heat generation or absorption has received little or no attention in the literature. Therefore, the main objective of this investigation is to analyze laminar natural convection in a partially heated porous enclosure from above by a uniform flux with internal heat generation. Thorough analysis of the effect of the internal heat generation/absorption on the heat transfer within the cavity will be carried out for various pertinent parameters such as internal Rayleigh number, Darcy number and porosity number.

2. Problem description and formulation

2.1 Geometry

Fig. 1 displays the schematic diagram of the two-dimensional enclosure considered in this study. A heat source with constant heat flux (q) is located on the bottom wall of the enclosure which is thermally insulated. The vertical walls and the horizontal top wall of the enclosure are maintained at a relatively low temperature (T_c). Furthermore, all thermo-physical properties of the fluid are taken to be constant except for the density variation in the buoyancy term, where the Boussinesq approximation is considered as follows:

$$\rho = \rho_0 [1 - \beta(T - T_0)] \quad (1)$$

Where ρ_0 is the fluid density at the reference temperature $T_0 = T_c$ and $\alpha = -\left(\frac{1}{\rho_0}\right)\left(\frac{\partial \rho}{\partial T}\right)_{p,c}$ is the thermal expansion coefficient.

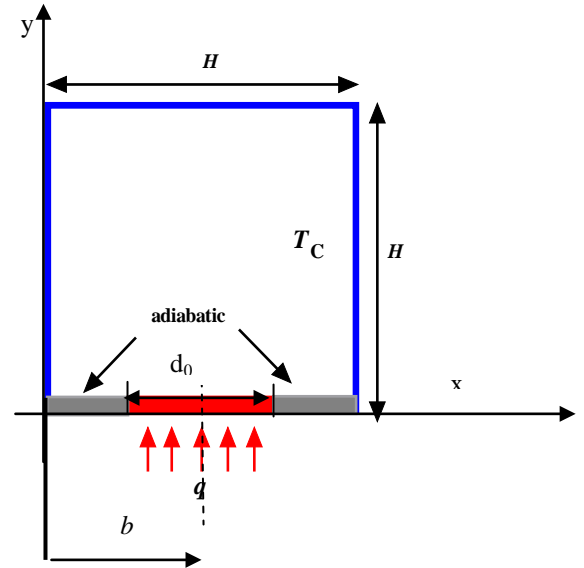


Fig1 Schematic diagram of the physical model

2.2 Equations

The continuity, momentum and energy equations for the laminar and steady state natural convection in the two-dimensional enclosure for a porous medium can be written as follows:

Continuity equation:

$$\frac{\partial U}{\partial X} + \frac{\partial V}{\partial Y} = 0 \quad (2)$$

X-momentum equation:

$$\frac{1}{\varepsilon} \left[\frac{\partial U}{\partial \tau} + U \frac{\partial}{\partial X} \left(\frac{U}{\varepsilon} \right) + V \frac{\partial}{\partial Y} \left(\frac{U}{\varepsilon} \right) \right] = -\frac{\partial P}{\partial X} - \frac{1}{Da} U + \frac{1}{\varepsilon} \left(\frac{\partial^2 U}{\partial X^2} + \frac{\partial^2 U}{\partial Y^2} \right) \quad (3)$$

Y-momentum equation:

$$\frac{1}{\varepsilon} \left[\frac{\partial V}{\partial \tau} + U \frac{\partial}{\partial X} \left(\frac{V}{\varepsilon} \right) + V \frac{\partial}{\partial Y} \left(\frac{V}{\varepsilon} \right) \right] = -\frac{\partial P}{\partial Y} - \frac{1}{Da} V + \frac{1}{\varepsilon} \left(\frac{\partial^2 V}{\partial X^2} + \frac{\partial^2 V}{\partial Y^2} \right) + \frac{Ra_E}{Pr} \theta \quad (4)$$

Energy equation:

$$\sigma \frac{\partial \theta}{\partial \tau} + U \frac{\partial \theta}{\partial X} + V \frac{\partial \theta}{\partial Y} = \frac{1}{Pr} \left(\frac{\partial^2 \theta}{\partial X^2} + \frac{\partial^2 \theta}{\partial Y^2} \right) + \frac{Ra_I}{Pr Ra_E} \quad (5)$$

Accordingly, foregoing equations introduce the following dimensionless parameters,

$$Ra_I = \frac{g\beta QH^3}{\nu \alpha k}, \quad Ra_E = \frac{g\beta \Delta TH^3}{\nu \alpha},$$

$$Gr = \frac{g\beta \Delta TH^3}{\nu^2}, \quad Pr = \frac{\nu}{\alpha}$$

Where ε is the porosity of the porous medium, Da is the Darcy number and σ is the ratio of heat capacities expressed respectively as:

$$Da = \frac{K}{H^2}; \quad \sigma = \frac{\varepsilon(\rho C_p)_f + (1-\varepsilon)(\rho C_p)_s}{(\rho C_p)_f}$$

The boundary conditions consist of no-slip and no penetration walls, i.e., $U = V = 0$ on all four walls. All dimensions are scaled to the length (H). The

non-dimensional values $x/H = X$, $y/H = Y$, $b/H = B$, and $d/H = d$. The dimensionless thermal boundary conditions, used to solve the Equations (2) – (5) are as follows:

$$U = V = 0 \text{ and } \theta = 0 \text{ for } X = 0 \text{ and } 0 \leq Y \leq 1$$

$$U = V = 0 \text{ and } \theta = 0 \text{ for } X = 1 \text{ and } 0 \leq Y \leq 1$$

$$U = V = 0 \text{ and } \frac{\partial \theta}{\partial Y} = 0 \text{ for } Y = 0 \text{ and}$$

$$0 \leq X \leq B - 0.5d$$

$$U = V = 0 \text{ and } \frac{\partial \theta}{\partial Y} = -1 \text{ for } Y = 0 \text{ and}$$

$$B - 0.5d \leq X \leq B + 0.5d$$

$$U = V = 0 \text{ and } \frac{\partial \theta}{\partial Y} = 0 \text{ for } Y = 0 \text{ and}$$

$$B + 0.5d \leq X \leq 1$$

$$U = V = 0 \text{ and } \theta = 0 \text{ for } Y = 1 \text{ and } 0 \leq X \leq 1$$

The local Nusselt number is defined at the discrete source by:

Here $\theta_s(X)$ denotes the dimensionless heat source temperature.

$$Nu(X) = \frac{1}{\theta_s(X)}$$

The average Nusselt number is computed by integrating $Nu(X)$ along the heat source of length d :

$$\overline{Nu} = \frac{1}{d} \int_{B-d/2}^{B+d/2} \frac{1}{\theta_s(X)} dX$$

3. Results and discussion

3.1 Effect of internal Rayleigh number (Ra_I)

A representative set of numerical results for the centerline temperature profiles ($Y=0.5$) versus the x abscissa are reported in Fig. 2. These figures illustrate the changes in the temperature profiles due to changes in the values of internal Rayleigh number for both internal heat generation and the absorption cases. The

presence of heat generation has the tendency to increase the temperature of the fluid in the center of the cavity when Ra_I is great than 10^5 . On the other hand, heat absorption produces the opposite effect; namely, decreases in the temperature. According to the generation case ($Ra_I > 0$), local Nusselt number slope vanishes for higher generation, indicating the significant role of the enhanced thermal properties of the porous medium in heat transport.

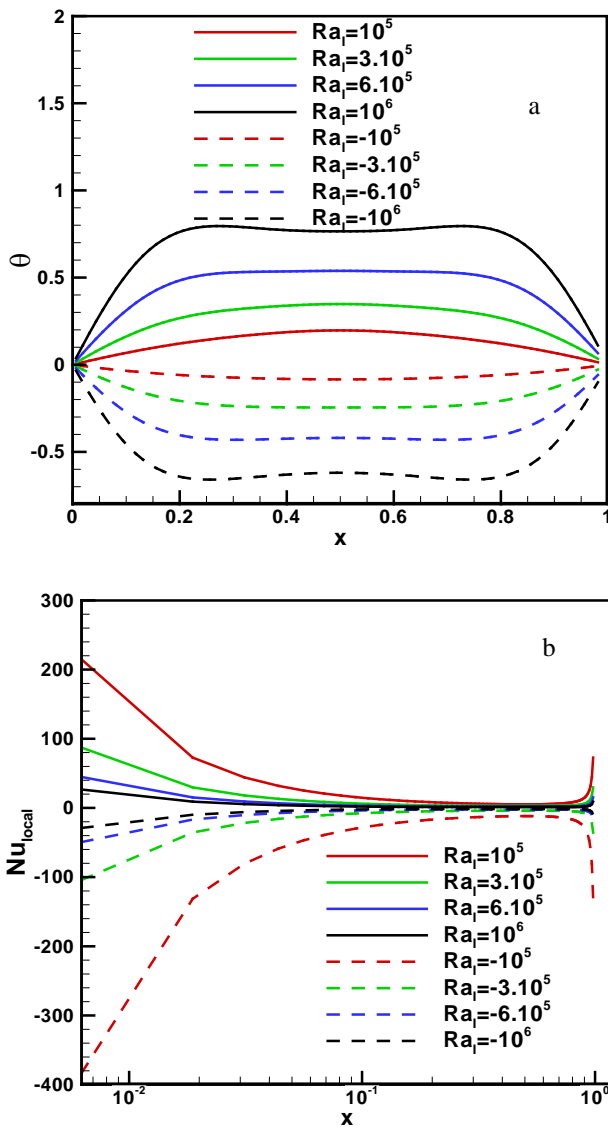


Fig2 Variation versus x abscissa of: (a) temperature centerline, (b) local Nusselt number, at various internal Rayleigh numbers for $d=0.5$, $Da=10^{-2}$ and $\epsilon=0.4$ ($Ra_I > 0$: generation; $Ra_I < 0$: absorption).

3.2 Effect of Darcy number on the heat transfer

In the following, we propose to quantify the heat transfer rate with the help of the average Nusselt number. For this purpose, Fig. 3 shows the variations of the average Nusselt number as function of the Darcy number for both heat generation and absorption case for various Ra_I numbers in range (-10^6) to 10^6 . The porosity (ϵ) of the porous medium is fixed to 0.4.

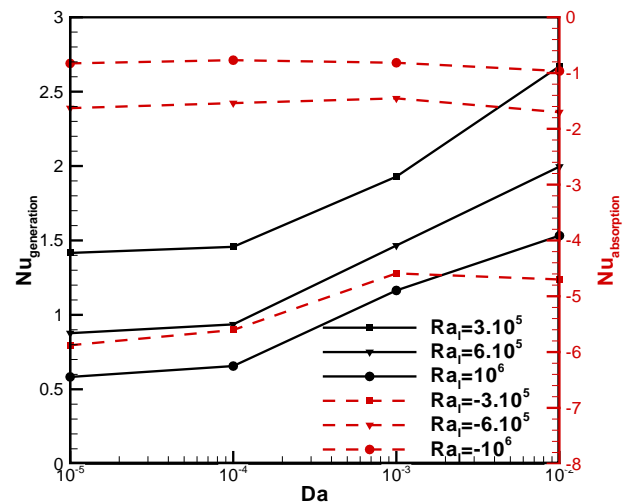


Fig. 3 Variation of average Nusselt number with Darcy number for $\epsilon=0.4$, $d=0.5$, $Ra_E=10^5$ and different internal Rayleigh numbers: generation (—), and absorption (---)

When the effect of the porous medium is referred, as it can be observed in this figure, Nu decreases as the Rayleigh number (generation or absorption) increases, while keeping the Darcy number constant. For a Darcy regime ($10^{-5} \leq Da \leq 10^{-4}$, $Ra_E=10^5$), Nu grows slowly keeping the internal Rayleigh number constant. This can be due to the fact that the velocities remain weak with a slightly permeable medium, which does not improve transfer. With the increase of Darcy number, according to the non-Darcy regime, the average Nusselt number increases due to the decrease of the heat source maximum temperature. This seems obvious since the average Nusselt number at the heat source is the inverse of the temperature along the source, higher

values of the average Nusselt number indicate decreased temperature. When the absorption case is concerned, the heat transfer rate remains almost constant while the absorption intensity is weak for both Darcy and non-Darcy regime. However, if the absorption intensity is augmented, there has been a rise in the heat transfer rate as the Darcy number increases.

3.3 Effect of porosity on the heat transfer

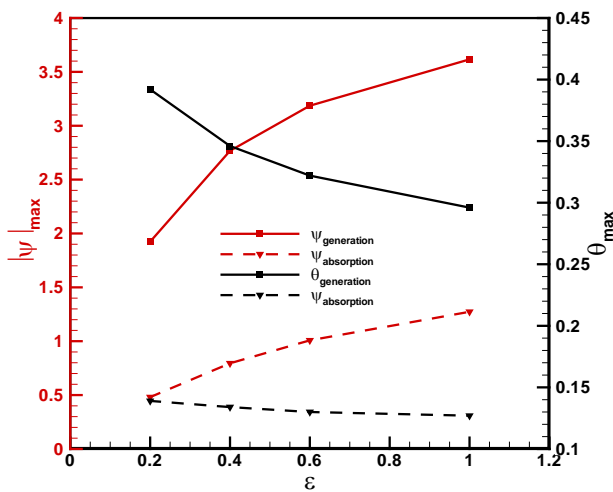


Fig. 4 Variation of the stream function and heat source maximum temperature (ψ_{max}) and (Θ_{max}), respectively, with porosity number for $d=0.5$, $Da= 10^{-2}$, $Ra_I=\pm 10^5$ and $Ra_E=10^5$.

Fig. 4 exhibits both the variation of stream function maxima ψ_{max} and maximum heat source temperature (Θ_{max}) versus the porosity number in range 0.2 to 1 according to the generation and absorption cases for $Da= 10^{-2}$ and $d=0.5$. The observations have been made with regard to the both maxima variations of stream function and heat source temperature versus ϵ . At this stage, we can conclude that the use of a porous medium instead of a homogeneous medium causes a significant cooling of the cavity both in the case of generation or absorption situation.

In Fig. 5, the variations of the average Nusselt number, for both internal heat generation and

absorption cases, are exhibited at a Darcy number of 10^{-2} , Rayleigh number Ra_E of 10^5 and different porosities.

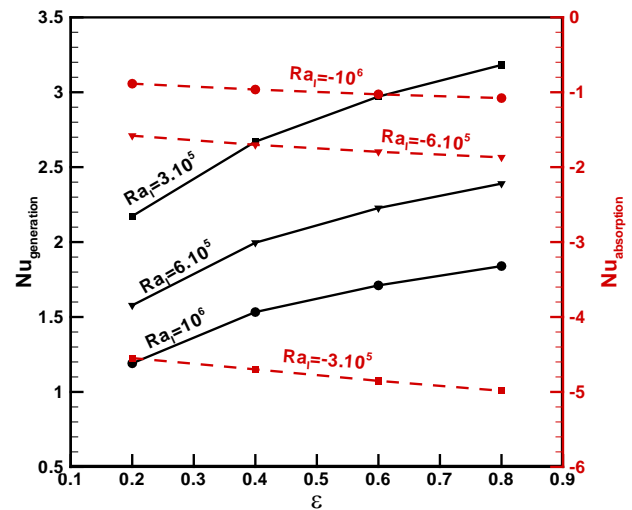


Fig. 5 Variation of average Nusselt number with porosity number for $Da=10^{-2}$, $d=0.5$, $Ra_E=10^5$ and different internal Rayleigh numbers: generation (—), and absorption (---)

It is observed that the heat transfer strength increases as the porosity of the medium is increased. Quantitatively, at $Ra_I=3 \times 10^5$ (non-Darcy regime), the average Nusselt number vary by 52% between the cases of $\epsilon=0.2$ and 0.8 . This enhancement can be explained by the fact that with an increase in the porosity coefficient, strength of convective motion increases because the medium tends to a homogeneous one where the fluid can circulates freely. As the internal Rayleigh number is decreased to lower values, the differences between the curves are perceptible. Therefore, even at lower Darcy numbers (not shown in figure), the variation of average Nusselt number with porosity is not negligible at lower internal Rayleigh numbers. Nevertheless, change in porosity hardly affects the average Nusselt number if the absorption process is considered. On the other hand, as the porosity of medium is increased, in Fig.5, we note that the differences between the curves of Nusselt number corresponding to different Ra_I are almost unchanged.

4. Conclusions

Extensive numerical results are reported on natural convection flow and heat transfer from a porous enclosure submitted to internal heat generation or absorption. The heat transfer behavior in the enclosure under consideration has been analyzed in the average Nusselt number. For all values of the considered Da , the stream function maximum (ψ_{max}) is found to increase with the increase in Da . However, the maximum of temperature at the heat source decreases slowly with the increase of the Darcy number. On the other hand, heat absorption produces the opposite effects. The magnitude of the circulating flow (ψ_{max}) grows when the permeability of the medium increases (Da) less significantly with respect to the absorption case. On other hand, accordingly to the internal generation case, the maximum circulating flow intensity is reached when the medium becomes saturate.

Optimal heat transfer rate is obtained for both high internal Rayleigh number and high porosity coefficient ($\epsilon=0.8$ and $Ra_1=10^6$). Note, however, that the lower heat transfer rate have been found in the first calculations ($\epsilon=0.4$ and $Ra_1=10^5$).

References

- [1] Ingham, D. and Pop, I., *Transport Phenomena in Porous Media III*, Elsevier Science, Oxford, 2005
- [2] Vafai, K., *Handbook of porous media*, 2nd ed, New York: Taylor & Francis; 2005.
- [3] Nield, D.A. and Bejan, A., *Convection in Porous Media*, third ed., Springer, New York, 2006
- [4] Brinkman, H.C., on the permeability of media consisting of closely packed porous particles, *Appl. Sci. Res.*, vol. 1, pp. 81–86, 1947.
- [5] Kuznetsov, A.V. and Nield, D.A., Thermal instability in a porous medium saturated by a nanofluid: Brinkman model, *Transp. Porous Med.*, vol. 81, pp. 409-422, 2010.
- [6] Nield, D.A. and Kuznetsov, A.V., Thermal instability in a porous medium layer saturated by a nanofluid, *Int. J. Heat Mass Transf.*, vol. 52, pp. 5796-5801, 2009.
- [7] Sankar, M., Bhuvaneswari, M., Sivasankaran, S., Do, Y., Buoyancy induced convection in a porous cavity with partially thermally active sidewalls, *Int. J. Heat Mass Transfer*, vol. 54, pp. 5173–5182, 2011.
- [8] Alloui, Z., Dufau, L., Beji, H., Vasseur, P., Multiple steady states in a porous enclosure partially heated and fully salted from below, *Int. J. Therm. Sci.*, vol. 48, pp. 521–534, 2009.
- [9] Mealey, L.R. and Merkin, J.H., Steady finite Rayleigh number convective flows in a porous medium with internal heat generation, *International Journal of Thermal Sciences*, vol. 48, pp. 1068–1080, 2009.
- [10] Reddy, B.V.K., Narasimhan, A., Heat generation effects in natural convection inside a porous annulus, *International Communications in Heat and Mass Transfer*, vol. 37, pp. 607–610, 2010.